Mem. S.A.It. Vol. 82, 726

Memorie della

Supernova remnants and pulsar wind nebulae in the Cherenkov Telescope Array era

M. Renaud for the CTA consortium

Laboratoire Univers et Particules de Montpellier, Université Montpellier 2, CNRS/IN2P3, CC 072, Place Eugène Bataillon, F-34095 Montpellier Cedex 5, France
e-mail: mrenaud@lupm.univ-montp2.fr

Abstract. The Cherenkov Telescope Array (CTA) is planned to serve as a ground-based observatory for (very-)high-energy gamma-ray astronomy, open to a wide astrophysics community, providing a deep insight into the non-thermal high-energy universe. It foresees a factor of ∼10 improvement in sensitivity above 100 GeV, with substantially better angular and spectral resolutions and wider field-of-view in comparison with currently operational experiments. The CTA consortium is investigating the different physics cases for different proposed array configurations and subsets. Pulsar Wind Nebulae (PWNe), the most numerous VHE Galactic sources, and Supernova Remnants (SNRs), believed to be the acceleration sites of the bulk of cosmic rays, will be two of the main observation targets for CTA. In this contribution, the main scientific goals regarding PWNe and SNRs are discussed, and quantitative examples of the capability of CTA to achieve these objectives are presented.

Key words. Gamma rays: general – Surveys – ISM: supernova remnants, cosmic rays

1. Introduction

While only a handful of sources were known to emit in the very-high-energy (VHE; E > 100 GeV) gamma-ray domain until 2005, more than 120 sources have now been detected (two third lying in the Galaxy)[1], thanks to the current generation of Imaging Atmospheric Telescopes (IACTs) such as H.E.S.S., VERITAS and MAGIC. The end-products of massive star evolution, Supernova Remnants (SNRs) and Pulsar Wind Nebulae (PWNe), are thought to be the main sites of particle acceleration, and are characterized by non-thermal emission over the entire electromagnetic spectrum through several mechanisms (synchrotron [SC], inverse-Compton [IC], non-thermal bremsstrahlung, proton-proton interactions and subsequent π^0 decay). The H.E.S.S. experiment, in particular, has imaged the shell-type morphology of several young ($\lesssim$ a few kyr) SNRs and has revealed a new population of middle-aged ($\gtrsim$ 10 kyr) VHE-emitting PWNe (Hinton & Hofmann 2009). Although these observations demonstrate that SNRs and PWNe are able to accelerate particles in the ∼10–100 TeV range, recent theoretical investigations have raised several issues on particle acceleration at (non-)relativistic shocks, within the general paradigm of the nature of the cosmic-ray (CR) sources in the Galaxy (see *e.g.* Blasi 2010).

Send offprint requests to: M. Renaud

[1] See http://tevcat.uchicago.edu/

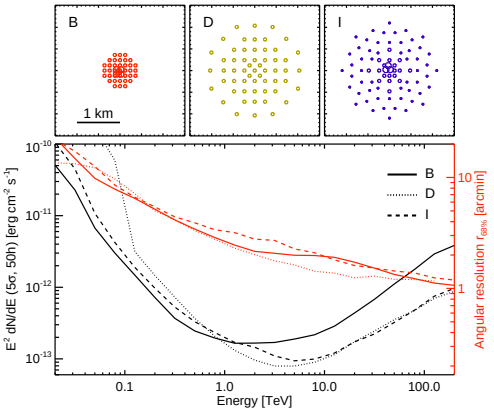

Fig. 1. *Upper panels:* Three representative CTA array layouts dubbed B, D and I. Telescope sizes are not drawn to scale. *Lower panel:* Point-source sensitivity (5 σ in 50 h, in black) and angular resolution (68% containment radius, in red) of the three configurations. B is optimized in the low-energy (< 1 TeV) domain, D provides the best sensitivity at energies > 1 TeV, and I is optimized for providing better performance over the whole energy range.

The Cherenkov Telescope Array (The CTA consortium 2010), currently under its Preparatory Phase (2011–2013), is an initiative to build an advanced facility for ground-based HE/VHE (20 GeV–200 TeV) gamma-ray astronomy, with various scientific themes, from cosmic energetic particles (origin of CRs, jets and shocks) to fundamental physics (Dark Matter, Lorenz Invariance violation). The consortium is firmly embedded in the European processes guiding fields of astronomy and astroparticle physics. It gathers $\gtrsim$800 scientists and engineers in $\gtrsim$100 institutes. The construction of the full array of 50–100 ~23–24 m-, ~10–12 m- and ~5–8 m-diameter Cherenkov telescopes is planned to be completed around 2018. The main characteristics of three representative CTA configurations, currently considered within the consortium, are presented in Figure 1. A point-source sensitivity at the level of one mCrab and an angular resolution of 1–2 arcmin at TeV energies are foreseen with such layouts. In the following, Monte-Carlo simulations of shell-type SNRs and PWNe as seen with CTA are presented, with an emphasis on spectro-imaging (§ 2) and population (§ 3) studies. The results presented here are based on simulations performed for observations at a zenith angle of 20°, assuming a symmetrical gaussian point spread function (PSF) with a 68% containment radius as given in Figure 1, while neglecting the effects of the finite energy resolution of the instrument (which are mitigated for the large energy ranges considered).

2. Spectro-imaging studies

RX J1713.7−3946 is the brightest shell-type SNR in the VHE domain, originally detected with H.E.S.S. (Aharonian et al. 2007), and more recently with *Fermi*/LAT in the HE domain (Abdo et al. 2011). The nature of the gamma-ray emission (IC emission from leptons vs. π^0 decay from hadrons) is still debated, even though IC emission seems to be favored from a spectral point of view. The joint *Fermi*/LAT and H.E.S.S. spectrum was fit with an exponential cutoff power-law in the form $N_0\ E^{-\Gamma}\ \exp(-(E/E_{cut})^{\beta})$. The best-fitted parameters have been used to simulate CTA spectra of RX J1713.7−3946 (whose morphology is assumed to be that measured with H.E.S.S., Aharonian et al. 2006), as shown in Figure 2 (left), for CTA-I and 50 h of observing time. Besides reducing greatly the uncertainties on each spectral parameter, CTA will be able to probe the highest energy domain. As shown by Morlino et al. (2009), and later confirmed by Ellison et al. (2010), the predicted IC emission from accelerated leptons, while accounting for the radio and X-ray measurements of the associated SC emission, could not explain the flux measured with H.E.S.S. above ~35 TeV (though with low S/N ratios of 2.5, 1.5 and 0.6). Therefore, any significant flux detected at the highest energies would point towards the existence of $\gtrsim$ 200 TeV hadrons still confined in the shell. For this purpose, 10^3 simulations of the RX J1713.7−3946 spectrum above 35 TeV in 50 h have been carried out. CTA-I/D are clearly favored over B, with mean S/N ratios of ~7 and 6, respectively.

Figure 2 (right) shows a CTA-I simulated image of RX J1713.7−3946 above 1 TeV in 50 h, assuming as the morphological and spectral templates the *XMM-Newton* im-

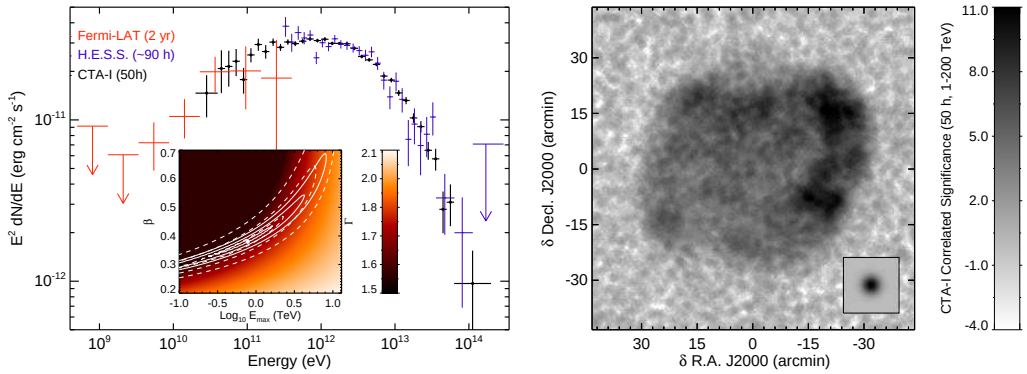

Fig. 2. CTA-I simulations of RX J1713.7−3946 for 50 h of observing time. *Left:* Spectral energy distribution (SED, in black) with the best-fitted parameters of the joint *Fermi*/LAT (in red) and H.E.S.S. (in blue) spectrum. The inset figure shows the 1, 2, and 3 σ confidence ellipses in the E_{cut}-β plane, derived from the fit of 100 simulated spectra (solid lines) and of the *Fermi*/LAT-H.E.S.S. spectrum (dashed lines), superimposed on the image of the Γ values. The white dot gives the best-fit values: $\Gamma \sim 1.62$, $E_{cut} \sim 0.78$ TeV and $\beta \sim 0.38$. *Right:* Correlated significance map ($R_{corr} = 0.02^\circ$) above 1 TeV. The *XMM-Newton* image of RX J1713.7−3946 (Acero et al. 2009) has been used as template. The CTA-I PSF is shown in the inset.

age (Acero et al. 2009) and the best-fit on the joint *Fermi*/LAT-H.E.S.S. SED, respectively. Spatial structures such as the double shell-like morphology in the W-NW region are clearly seen. Simulated spectra have also been extracted over 0.25°-wide boxes, as defined in Aharonian et al. (2006). The mean errors on Γ and E_{cut} (with β fixed) are estimated to be of the order of 0.08 and 0.3 TeV (90% confidence level), respectively, *i.e.* small enough to allow the exploration of possible azimuthal variations of these parameters, in combination with what is performed nowadays in X-rays on the SC spectrum of many young SNRs.

3. Population studies

On one hand, the small number of detected TeV shells (RX J0852−4622 aka Vela Jr, RX J1713.7−3946, RCW 86, SN 1006 and HESS J1731−347) prevents one from performing population studies in order to shed further light on particle acceleration in these sources, even when considering the other (unresolved) detected young shell-type SNRs (such as Cas A and Tycho). On the other hand, ∼30 VHE PWNe have been detected so far, mainly in the inner regions of the Galaxy surveyed with H.E.S.S., most of them being extended on scales of $\sigma \sim 0.2^\circ$. Moreover, a significant fraction of the unassociated VHE sources could be such ancient nebulae, as suggested by de Jager et al. (2009). This scenario seems to be conforted by the on-going detection of many gamma-ray pulsars with *Fermi*/LAT, several of which lying close to VHE sources (*e.g.* MGRO J1908+06/PSR J1907+0602, Abdo et al. 2010). It is then worth estimating the expected number of shell-like SNRs and PWNe to be detected with CTA, in order to (1) trigger SNR/PWN population studies and (2) quantify the level of source confusion along the Galactic Plane (and especially in the regions close to the spiral arm tangents), given the large number of already-detected VHE PWNe and PWN candidates. In the following, simulations have been carried out assuming a reasonable exposure time of 20 h in the survey of the Galactic Plane.

For this purpose, three shell-type SNRs (RX J1713.7−3946, Vela Jr, RCW 86) and three PWNe (G21.5−0.9, Kes 75, HESS J1356−645) were considered to be representative of the SNR/PWN Galactic populations in the VHE domain. Their morphological and spectral characteristics, as measured with H.E.S.S., together with their respective distance estimates, have been used

to simulate sources throughout the inner ($|\ell|$ < 60°, $|b|$ < 5°) Galaxy (see Figure 3, upper panels). The horizon of *detectability* is defined as the distance at which the source has a peak significance of 5, while the horizon of *resolvability* (for shell-type SNRs) represents the distance up to which a shell-type fit on the source radial profile (see Figure 3, bottom) is favored at ≥ 3 σ over a simple gaussian fit (*i.e.* the shell is identified as such, and statistically favored over a PWN-like shape). These two horizons can be translated into fractions of the total number of detectable/resolvable sources with CTA, based on a model of the Galactic source distribution. The logarithmic spiral arms model of Vallée (2008) is assumed, with a galactocentric distribution given by Case & Bhattacharya (1998), and an arm dispersion as a function of the galactocentric radius following the Galactic dust model of Drimmel & Spergel (2001)[2]. The resulting source distribution is shown in Figure 4, together with the fraction of visible[3] SNRs and PWNe as a function of the distance to the Sun.

As seen in Figure 4 (middle), a large fraction f_{SNR} (∼0.3–0.9) of RXJ1713-, VelaJr- and RCW86-like Galactic SNRs should be *detectable* with CTA-I/D (both configurations being definitively favored in comparison to B, discarded in the following), but only a small fraction of them (∼0.1–0.2) would actually be *resolvable*. Although the timescale (τ_{SNR}) during which a SNR shines in the VHE domain is very sensitive to many parameters (related to the stellar progenitor, the acceleration process and the ambient medium), it is assumed to be identical among all the SNRs. Therefore, the fractions given above are converted into numbers following $N_{SNR} \sim 75\ f_{SNR}\ (\tau_{SNR}/3\mathrm{kyr})\ (\nu_{SN}/2.5)$, where ν_{SN} is the Galactic SN rate (in SNe per century, see Li et al. 2011). This leads to ∼20–70 detectable TeV SNRs, among which ∼7–15 would be resolved with CTA-I/D. The same simulations have been carried out by improving the CTA PSF by a factor of 2 (*i.e.* $\lesssim 1'$ at 1 TeV, see Figure 1) in order to quantify the effect of the angular resolution on the number of detectable (N_{detect}) and resolvable (N_{resolv}) SNRs. While N_{detect} gets larger by only 20% at most, N_{resolv} increases by a factor of (1.5–1.9).

As for PWNe, a large fraction f_{PWN} (∼ 0.4–0.8) of G21.5-, HESSJ1356- and Kes75-like nebulae should be detectable with CTA-I/D (see Figure 4, right). de Jager & Djannati-Ataï (2009) have estimated the lifetime of TeV-emitting leptons in such sources to be ∼40 kyr (for B = 3 μG, similar to what has been found in several PWNe such as Vela X). This gives $N_{PWN} \sim 800\ f_{PWN}\ (\tau_{PWN}/40\mathrm{kyr})\ (\nu_{PSR}/2)$, and implies that ∼ (300–600) PWNe should be detected with CTA-I/D. Again, these estimates should be taken with care as they do not account for any time evolution of the TeV luminosity in these sources, which itself depends on many parameters (*e.g.* Gelfand et al. 2009).

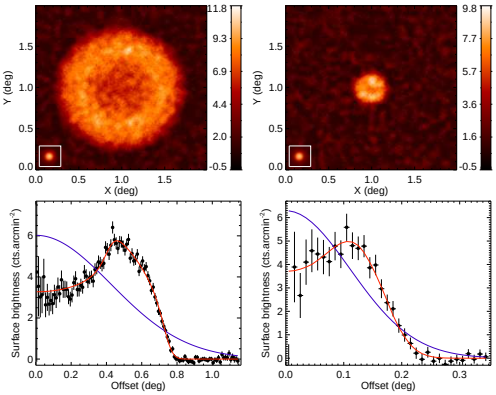

Fig. 3. *Upper panels:* CTA-I simulated images of RX J1713.7−3946-like SNR located at 1 (left) and 4 (right) kpc. The color bars give the correlated significance, and the CTA-I PSF is shown in the insets. *Lower panels:* Radial profiles of the VHE surface brightness at 1 (left) and 4 (right) kpc. The blue and red lines represent the best-fit curves for uniform-sphere and shell-type morphologies, respectively.

4. Conclusions

In this contribution, simulations of Galactic shell-type SNRs and PWNe in the VHE domain as seen with CTA have been presented,

[2] With regard to PWNe, any potential displacement from pulsar birth place due to the kick velocity has been ignored.

[3] The visibility is defined here as the fraction of the sky seen by an observatory located at the same latitude as the H.E.S.S. site, at zenith angles ≤ 45°.

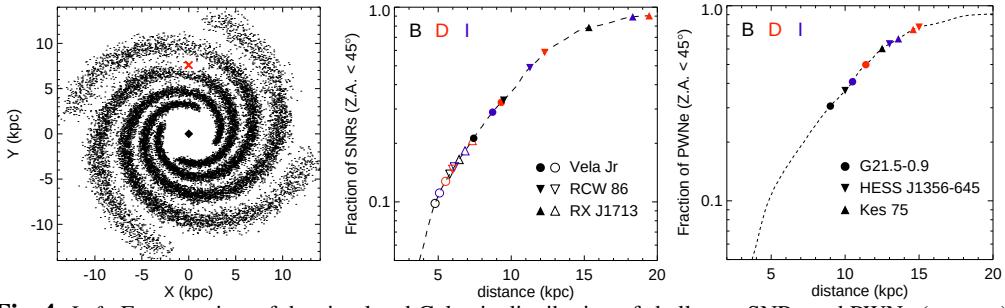

Fig. 4. *Left:* Face-on view of the simulated Galactic distribution of shell-type SNRs and PWNe (see text). The Sun and the Galactic Center are marked with a red cross and a black diamond, respectively. *Middle:* Fraction of visible shell-type SNRs as a function of the distance to the Sun. For each source and each CTA configuration considered here, filled and open symbols give respectively the horizons of detectability and resolvability, as defined in the text. *Right:* Same as the middle figure, for the three considered PWNe.

for three different array configurations. As shown above, the configurations optimized at very-high energies (> 1 TeV) are clearly favored with respect to these two source classes. This is naturally the case for probing the nature of the highest-energy gamma-rays in the brightest SNRs such as RX J1713.7−3946 (and more generally for seeking in the $\gtrsim 100$ TeV domain the so-called Galactic PeVatrons, *i.e.* sources of CRs with energies close to the knee at ~ 3 PeV). Moreover, first estimates of the number of detectable/resolvable SNRs and PWNe have pointed out the twofold importance of the angular resolution, in order to (1) pinpoint the shell-type morphology of SNRs and (2) mitigate the source confusion in the inner regions of the Galactic Plane, given that hundreds of PWNe are expected to be revealed with CTA. For this purpose, an angular resolution of $\lesssim 1'$ at TeV energies seems to be desirable, although more quantitative estimates of the source confusion need to be carried out. As for the former point, it turns out that, regarless of the final instrument PSF, a large fraction of the detected shell-type SNRs will not be identified as such based on solely their VHE morphology. Therefore, follow-up multi-wavelength observations with the on-going or planned facilities (EVLA, LOFAR, eROSITA, NuSTAR, ASTRO-H), towards these potential CR sources will be of crucial importance.

Acknowledgements. I thank all the members of the CTA-PHYS working group for valuable discussion and helpful comments on the manuscript. We gratefully acknowledge support from the agencies and organisations listed in this page: http://www.cta-observatory.org/?q=node/22.

References

Abdo, A. A. et al. (*Fermi*) 2010, ApJ, 711, 64
Abdo, A. A. et al. (*Fermi*) 2011, ApJ, 734, 28
Acero, F., et al. 2009, A&A, 505, 157
Aharonian, F. et al. (H.E.S.S.) 2006, A&A, 449, 223
Aharonian, F. et al. (H.E.S.S.) 2007, A&A, 464, 235
Blasi, P. 2010, Proceedings of ICATPP, in press, arXiv:1012.5005
Case, G. L., & Bhattacharya, D. 1998, ApJ, 504, 761
de Jager, O. C., et al. 2009, Proceedings of 31st ICRC, in press, arXiv:0906.2644
de Jager, O. C., & Djannati-Ataï, A. 2009, Neutron Stars and Pulsars, ASSL, Vol. 357, pp. 451
Drimmel, R., & Spergel, D. N. 2001, ApJ, 556, 181
Ellison, D. C., et al. 2010, ApJ, 712, 287
Gelfand, J. D., Slane, P. O., & Zhang, W. 2009, ApJ, 703, 2051
Hinton, J.A., & Hofmann, W. 2009, ARA&A, 47, 523
Li, W. et al. 2011, MNRAS, 412, 1473
Morlino, G., Amato, E., & Blasi, P. 2009, MNRAS, 392, 240
The CTA consortium, 2010, arXiv:1008.3703
Vallée, J. P. 2008, AJ, 135, 1301